

Time Resolved Cryo-Correlative Light and Electron Microscopy

Gréta V. Szabo and Thomas P. Burg*

Complex materials exhibit fascinating features especially in situations far from equilibrium. Thus, methods for investigating structural dynamics with sub-second time resolution are becoming a question of interest at varying spatial scales. With novel microscopy techniques steadily improving, the temporal and spatial limits of multiple imaging methods are investigated with an emphasis on the important role of correlative imaging and cryo-fixation. A deep-dive is taken into cryo-correlative light and electron microscopy (CLEM) as a starting point for multimodal investigations of ultrastructural dynamics at high spatiotemporal resolution. The focus is on highlighting the different microscopy methods that capture the following key aspects: 1) samples are as close to native state as possible 2) dynamic process information is captured, 3) high structural resolution is enabled. Additionally, the size of samples that can be imaged under these conditions is looked at and approaches not only focusing on single molecules, but larger structures are highlighted.

1. Introduction

Microscopic observations provide valuable insight into the spatial structure of complex materials. As microscopy with photons, charged particles, and mechanical probes reaches new heights of sensitivity and resolution, sample preparation plays an increasingly critical role. Soft materials and materials comprising light elements are sensitive to damage and often provide low intrinsic contrast. For decades, cell and structural biologists have perfected imaging techniques for such fragile specimens with astonishing success. The discovery that vitrification in cryogenic liquids can preserve the native structure of biological samples for imaging

under vacuum laid the foundation for the field of electron cryomicroscopy (cryo-EM). Some of these methods are increasingly adopted by materials scientists, for example to investigate the structure of solid–liquid interfaces in battery research and catalysis, or to reveal the morphology of organic nanoparticles.

Understanding the transformations and intermediate states far from equilibrium is often of great interest. Such investigations are enabled by two approaches, which may be combined: First by continuous live imaging and second by using time resolved methods to prepare and stabilize transient states. In light microscopy (LM), dynamic, or live imaging, is routine. Super-resolution LM (SRLM) techniques like Stimulated Emission Depletion microscopy (STED), Stochastic Optical

Reconstruction Microscopy (STORM), Photoactivated Localization Microscopy (PALM), structured illumination microscopy (SIM) and Minimal photon FLUX microscopy (MINIFLUX) allow for spatial resolution far below the Abbe limit of ≈ 100 nm. However, time resolution is limited by the rate of photon collection, which is constrained by photophysics and by the photochemical degradation of dyes under intense illumination. Thus, imaging wide fields at high resolution can take multiple seconds to minutes. Other methods, like atomic force microscopy (AFM) do not need fluorescent probes, but they only provide topographic images. Electron microscopy (EM) provides spatial resolution down to the Angstrom-scale, but conventional EM is limited to imaging static objects.

To enable dynamic structural imaging with high resolution, some exciting developments are underway. In one approach, samples are enclosed in vacuum-tight, electron transparent gas or liquid cells, which can be introduced directly into electron or X-ray beams. This method has intriguing potential for imaging non-equilibrium processes. Several excellent reviews have tracked the latest developments in this field.^[1,2]

In another approach, which is exemplified by dynamic CLEM, a process is first observed and/or triggered dynamically, e.g. during live imaging in the light microscope (LM). Then a state is fixed after a set delay and imaged at high resolution in the electron microscope (EM). The mode of fixation plays a crucial role. Chemical fixation and cryofixation are available. Chemical fixatives are routinely used in biological microscopy to preserve cells for imaging. However, chemical fixatives are often cytotoxic and deform the ultrastructure by dehydration

G. V. Szabo, T. P. Burg
Department of Electrical Engineering and Information Technology
Technische Universität Darmstadt
64283 Darmstadt, Germany
E-mail: thomas.burg@tu-darmstadt.de
T. P. Burg
Centre for Synthetic Biology
Technische Universität Darmstadt
64289 Darmstadt, Germany

 The ORCID identification number(s) for the author(s) of this article can be found under <https://doi.org/10.1002/adfm.202313705>

© 2024 The Authors. Advanced Functional Materials published by Wiley-VCH GmbH. This is an open access article under the terms of the [Creative Commons Attribution](https://creativecommons.org/licenses/by/4.0/) License, which permits use, distribution and reproduction in any medium, provided the original work is properly cited.

DOI: 10.1002/adfm.202313705

Supporting Information and cross-linking.^[3] Cryofixation provides outstanding structural preservation when cooling is performed at a high enough rate to avoid ice crystallization. Yet, this process, which is also known as vitrification, is technically more complex than chemical fixation and requires sophisticated instrumentation.

There have been several recent reviews on different aspects of cryo-CLEM. Focus of these is often around cryo-preparation methods,^[4,5] gaps and advances in cryo-EM, including some aspects of temporal dynamics^[6-10] review on cellular process investigation in native state,^[11,12] or review of opportunities of correlative EM or ET.^[13-15] These all show the growing interest in cryo-CLEM over the last years.

The aim of this perspective is to deep-dive on the current state and future prospects of dynamic cryo-CLEM methods, deciphering its temporal resolution limits, as well as highlighting general limitations and future opportunities. First, an overview on methods available for dynamic imaging and their prominent use cases is given. The second part focuses on methods for imaging dynamic processes and their spatiotemporal limits through novel correlative methods we consider most promising (not exclusively cryo-CLEM approaches). We discuss current limitations given by different cryo-fixation methods on nativity, sample size, and cooling rates. In the third section, dynamic cryo-CLEM approaches we consider as very promising for future biological observations are clustered along six promising methodologies: a) conventional cryo-CLEM. b) rapid sample transfer. c) triggered stimulation. d) chemical fixation of sample during observation. e) cryo-arrest under observation from stable warm equilibrium to stable cold equilibrium. f) cryo-arrest under observation, from unstable warm equilibrium to stable cold equilibrium. We discuss the principles, spatiotemporal boundaries, advances, and limitations of each of the methods in depth.

2. In Situ Imaging at High Spatial and Temporal Resolution

Conventional light microscopy can image dynamics at video rates (tens to hundreds of frames per second), with limitations mainly imposed by image brightness and detector sensitivity (Figure 1A – yellow cell sample). Spatial resolution is limited by the Abbe diffraction limit to a few hundred nanometers ($d \cong \frac{\lambda}{2n \sin \alpha}$, where λ is the wavelength, $n \cdot \sin \alpha$ the numerical aperture).^[16] To observe dynamic processes with higher spatiotemporal resolution in the far field using visible light, novel SRLM techniques need to be employed. For example, STED, PALM, STORM and SIM super-resolution techniques all provide spatial resolution in the ≈ 10 –100 nm range. Temporal resolution, on the other hand, varies widely. Through methods like MINIFLUX, the times necessary for pinpointing single molecules with nanometer precision can be reduced to hundreds of microseconds, and with novel SIM techniques^[17-19] or large-scale parallelization,^[20] tens to hundreds of micrometer large fields of view have been imaged at video rates. Despite these advances, imaging wide fields of view will often push the time resolution to the range of seconds, due to the limited photon flux, finite blinking rates, and/or finite activation times of fluorescent molecules^[21-23]

Other methods, like atomic force microscopy (AFM), (soft) X-ray imaging or liquid cell electron microscopy (LCEM) allow investigations at nanometer resolution without fluorescent labels. However, AFM can only be used on surfaces that are directly accessible to nanomechanical probes. In addition, probe-sample interactions may interfere with the system unless it is fixed or frozen. Using X-rays also enables nanoscopy by pushing the Abbe limit further than visible light. Soft X-rays are specifically interesting for live cell imaging due to a theoretical diffraction limit in the scale of a few nanometers combined with tens of micrometers penetration depth and useful absorbance contrast in biological samples and soft materials.^[24] The high doses needed to image aqueous samples, however, may cause sample toxicity or structural changes.^[25] LCEM is a technology that allows observation of aqueous samples with EM by encapsulating probes into small sample holders in their aqueous state. While promising for many applications, in situ EM like X-ray imaging requires great attention to detail and high-quality controls to rule out artefacts due to the intense ionizing radiation.^[26] Especially with prolonged illumination times, sample toxicity increases and sub-structures can be destroyed.^[27] Moreover, temporal sampling issues and motion blur need to be considered. Thus, while super-resolution microscopy, AFM, X-ray microscopy, and LCEM enable powerful dynamic observation with high spatial resolution, all these methods also possess limitations. Therefore, it is interesting to consider precision-timed fixation in some situations as an alternative for obtaining dynamic information.

Below, we will discuss dynamic CLEM to illustrate the case. The combination of dynamic (i.e., live) LM and EM is highlighted as one representative of a wider class of correlative analytical methods to investigate both the kinetics and the intermediate states of a system. For example, cryo-EM can reach a spatial resolution of tens of Angstroms with spherical aberration correction and direct electron detectors, but cryo-EM does not allow for dynamic imaging by itself^[28] (Figure 1B). We use the term *dynamic* correlative light and electron microscopy (dynamic CLEM) to emphasize a combination of LM and EM by which live imaging is performed just before, and sometimes up to, the exact time of fixation to fill this gap. The precise synchronization of an applied trigger or stimulus and fixation can sometimes provide additional dynamic insight. If the experiment is repeated with different delays, a time course can be reconstructed, potentially with millisecond temporal resolution, as will be detailed later (Figure 1C). For biological samples, the approach can be advantageous by highly limiting sample toxicity. In materials science, it provides an interesting complement to LCEM. For example, time resolution matters greatly in research on crystallization processes, new battery materials, or investigations of the intermediate states of electrocatalysts.^[15] However, the confines of an EM liquid cell holder can sometimes be too narrow to incorporate such systems into LCEM, even in a minimal form.

3. Fixation of Biological and Soft Materials for Electron Microscopy: Principles and Limitations

There are three broad categories of preparing biological and soft materials for the electron microscope: native state (no fixation), chemical fixation, and numerous variants of cryo-fixation. Taking a brief look at these is essential to understanding the possibilities

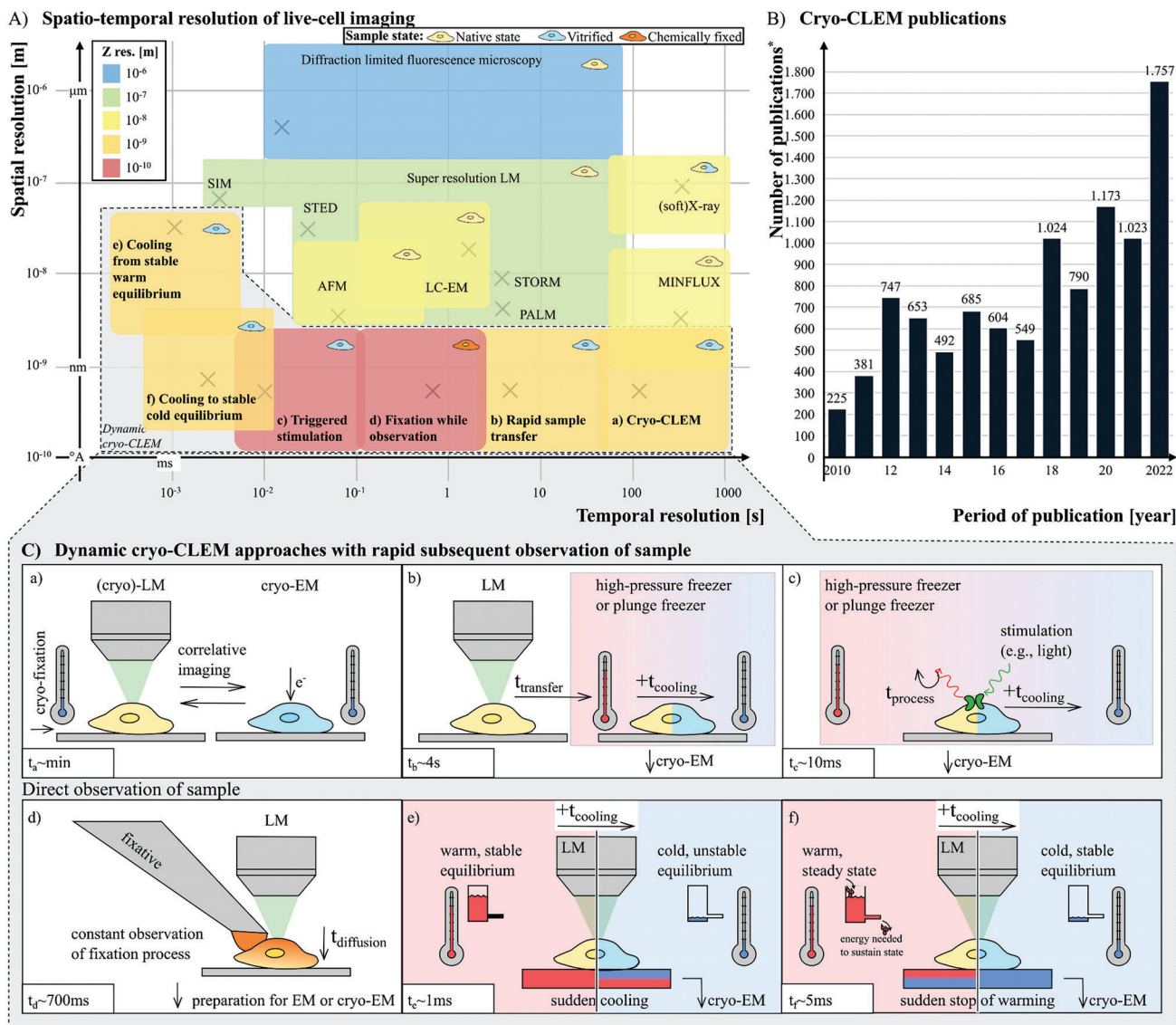


Figure 1. A) Typical spatiotemporal resolution and sample nativity for microscopy techniques with examples: Diffraction limited fluorescence microscopy (≈ 10 ms, ≈ 500 nm),^[30] Native state techniques (with yellow cell) Super-resolution light microscopy – entire image, not single molecule: STED (35 ms, 62 nm),^[21,72] PALM (3 s, ≈ 10 nm),^[31,73] STORM (3 s, 60 nm),^[23] SIM (≈ 1 ms, 60 nm),^[19] (Soft)-X-ray (\approx min, ≈ 100 nm),^[32,75] Liquid cell electron microscopy (LC-EM) (3 s, 35 nm),^[26,76] Atomic force microscopy (AFM) (≈ 80 ms, ≈ 2 nm),^[33,74] MINFLUX (0.1 ms (for single fluorophore tracking) – 40 min (for image), 1–3 nm),^[34] Dynamic cryo-EM techniques: a) conventional cryo-CLEM (> 10 s, \approx nm),^[35] b) rapid sample transfer from live LM to sample cooling (e.g., high-pressure freezer or plunge freezer) and cryo-EM,^[36] c) triggered stimulation and rapid cryo-arrest (10 ms, \approx nm),^[37] d) fixation of sample while observation, later cryo-substitution and cryo-EM (700 ms, \approx nm),^[6,77] e) cooling of sample from stable warm equilibrium to unstable cold equilibrium (1 ms, 80 nm),^[38] f) cooling of sample from unstable warm equilibrium to stable cold equilibrium (5 ms, \approx nm)^[39] Details in table in appendix. B) Number of publications on correlative cryo-electron microscopy based on full text search^[40] C) Schematic principle of methods for dynamic process observation for cryo-CLEM, current best experimental dynamic temporal resolutions achieved a) tracing back dynamics by correlating (cryo)-LM with (cryo)-EM: timescales of minutes.^[41] b) rapid sample transfer from live LM to sample cooling (e.g., high-pressure freezer or plunge freezer) and cryo-EM.^[36] c) triggered (e.g., light, electrical, chemical) stimulation and rapid cryo-arrest of sample.^[42] d) chemical fixation of sample during observation.^[6] e) Cryo-arrest of sample during observation, from warm equilibrium state to cold equilibrium state using highly thermally conductive materials.^[38] f) Cryo-arrest of sample during observation, from warm non-equilibrium state to stable cold equilibrium state.^[39]

for dynamic observation. It should be noted that in this perspective we focus on the aspects of fixation without differentiating for which type of electron microscopy (SEM, TEM, STEM, FIB/SEM, etc.) samples are destined. The key aspects of vacuum compatibility, electron transparency/accessibility, and radiation hardness are similar in all cases.

First, as described in more detail above, real-time imaging of hydrated biological/soft materials at room temperature in the electron microscope is possible through liquid cell techniques, but the high electron dose leads to sample toxicity and deformation,^[10,26] Thus, the second and perhaps most widely used approach is to stabilize samples using chemical fixation.

Table 1. Overview of sample thickness and cooling rate. Freezing through submerging in cold liquid: experimental data from,^[48,49] theoretical boundary from;^[50] Freezing through moving sample to cold surface: Experimental data from,^[51] theoretical boundary from^[52] (sample size based on 40 pl droplets); freezing through turning off heating with cold sink below sample: experimental data from,^[53] theoretical boundary from;^[54] sudden cooling of sample holder: data from;^[38] high pressure freezing: experimental data from,^[55] theoretical boundary from.^[56]

Cooling type	Cryo-fixation method (e.g.,)	Exp. max. thickness ^[μm]	Cooling rate ^[K s⁻¹]	Ice conditions	Theo. max thickness ^[μm]	Cooling rate ^[K s⁻¹]	Simulation conditions	Sample thickness ratio
In fluid	Submerging in cold liquid (plunge-, spray-freezing)	≈<0.1–1	–	3–5 nm ice crystal formation	≈0.2	10 ⁸ –10 ¹¹	Cooling of water between two ethane layers	
On surface	Moving sample to cold surface (slam freezing, super flash freezing)	10–30	8.5–55 × 10 ⁴	Ice micro-crystals at 12–30 μm depth	≈30	0.72–2.2 × 10 ⁴	40 μm droplet sizes on cold surface	
	Turning off heating with cold sink below sample (microfluidic freezing)	≈20	2 × 10 ⁴	Some crystals in EM and cryoprotectants	≈15	10 ⁵ –10 ⁶	Microfluidic layer of 0.5 to 5 μm between heater and cells	
	Sudden cooling of sample holder (cooling of heat exchanger)	≈50	0.4–1.2 × 10 ⁴	No visible ice crystals in LM	≈13–50	10 ⁴ –10 ⁵	Middle of 100 μm thick sample on diamond	
With pressure	High pressure freezing	≈200–600	5 × 10 ² –5 × 10 ³	10–15 nm ice crystal formation	≈200	1–6 × 10 ³	Slam freezing 200 μm z depth at 210MPa	

Though many chemical fixatives exist – physical agents (e.g., heat), aldehydes (e.g., formaldehyde, glutaraldehyde), coagulants (e.g., methyl alcohol), oxidizing agents (e.g., osmium tetroxide), and others – they are cytotoxic to different degrees or deform the ultrastructure of cells.^[3] The third approach, which has been gaining widespread popularity with the emergence of cryo-EM, is vitrification with or without the use of cryoprotectants. Vitrification, i.e., the solidification of a liquid in a glassy, amorphous structure, occurs when the substance is cooled rapidly below its glass transition temperature. For pure water, the homogeneous ice nucleation temperature at atmospheric pressure is $T_v \approx 235$ K, and vitrification happens below the glass transition temperature of $T_g \approx 136$ K.^[29] The critical cooling rates can be calculated through $CCR = \frac{\Delta T}{\Delta t}$.

The critical cooling rates (CCR) for pure water have been theoretically estimated to lie between 3×10^6 ^[43] and 1×10^{10} K s⁻¹.^[44] Although such extreme rates cannot usually be attained experimentally, vitrification can still be achieved in many biological and synthetic samples of great relevance. In biological specimens, this is possible because one does not deal with pure water but with solutions containing electrolytes and biomolecules that provide some cryoprotection themselves. Cells, in addition, seem to have a tolerance for small ice nucleation (<1 μm),^[45] even though possible long-range artefacts introduced by seemingly localized crystallization require careful consideration on a case-by-case basis. Taking into account these observations, estimates have been made that $CCR \approx 10^4$ K/s are necessary.

There are different ways of cooling down samples. The most frequently used one is plunge freezing, where a thin layer of a liquid sample on a TEM grid is plunged into liquid ethane. The sample thickness with this approach is in practice limited to between ≈100 nm and a maximum of ≈1 μm to allow for sufficient cooling rates (Table 1). The second cluster of approaches uses contact to cold surfaces instead of cold liquids. Approaches vary from printing on cooled surfaces, active heating of the sample against a cold heatsink and ultrarapid cooling of the sample holder with the samples already on it. While the methods do vary,

a universal limitation of these techniques remains that vitrification is attainable only for samples up to a maximum thickness on the order of 10 μm, at least in aqueous systems (Table 1). To vitrify thicker samples, either cryo-protectants need to be used, or the sample needs to be frozen at high pressure. Cryoprotectants decrease the rate requirement for cooldown, but they also influence the nativity of samples. High pressure freezing (HPF) at 2000 bar relaxes the critical cooling rate without cryoprotectants to ≈10³ K s⁻¹ and allows for increased sample thickness in the range of a few hundred micrometers (Table 1).

While there are clear advantages to high-pressure freezing, such as the increased permissible sample thickness and size without the use of additional cryo-protectants, perfect ultrastructural preservation is not guaranteed. For example, it has been observed that the local continuous twist between some molecules is modified, long-range cholesteric stratification disappears, and the characteristic macro ripple-phase of two-component liposome systems is drastically changed.^[46,47]

In conclusion, samples ranging from ≈100 nm to ≈100 μm can be cryo-fixed with different methods providing good structural preservation without cryoprotectants. Plunge freezing is suitable for samples ≈100 nm to 1 μm thick. Slam freezing samples on cryogenically cooled surfaces can produce well-preserved samples ≈10x thicker, in the range of 10 μm. Finally, HPF can preserve the ultrastructure of samples that are thicker yet by a factor of ten, reaching into the regime of ≈100 μm. (Table 1). These considerations should be kept in mind, when further evaluating cryo-CLEM approaches and their potential.

4. Dynamic CLEM Techniques

Being able to arrest dynamic processes with high timing accuracy and precision can offer an attractive solution when true real-time imaging is not feasible for the described reasons. Especially dynamic cryo-CLEM methods, which combine pre-fixation live imaging with time-resolved cryo-fixation, are promising due to their superb structural preservation and the rapid, homogeneous

arrest of dynamics throughout the sample by ultra-rapid cooling. We propose to classify dynamic CLEM methods into six unique groups. These are given below, with the theoretical idea, current best results, and application perspectives (Figure 1C).

- a) **Conventional cryo-CLEM:** Correlation of light microscopy and electron microscopy of cryogenically frozen samples is a fast progressing field. First approaches to obtain dynamic information relied on the identification of discrete states based on the morphology of the fixed object. For example, phase changes between growth and shrinkage of microtubules have been observed in this manner.^[57] Since then, the use of cryo-CLEM has vastly expanded (Figure 1B) and many groups started to work on enhanced localization of areas of interest (e.g., through correlative lamellae preparation) and on closing the temporal gap between light microscopic observation, cryo-arrest and cryo-EM using rapid transfer and in situ techniques.^[58–60] Without these, however, dynamic cryo-CLEM is limited to relatively slow processes with typical timescales in the range of minutes with well-characterized morphologies.
- b) **Rapid sample transfer:** The first approaches to not only correlate, but to capture specific events occurring live in the light microscope focused on rapid sample transfer by moving the sample from the light microscope quickly to a cryofixation device. The rapid transfer system developed by Verkade et al. for high-pressure freezing (HPF) marked a milestone in this field. Dynamic processes, such as the fusion of multivesicular bodies, could be observed live in the light microscope and relocated later in the EM with an effective time lapse of ≈ 4 s between live imaging and HPF.^[36] Rapid transfer in ≈ 1 s is nowadays possible with the latest generation of HPF technology, for example the Leica ICE and the CryoCapCell Live μ . Koning et al. attained a similar time resolution by rapid transfer to plunge freezing with a system known as MAVIS.^[61,62] The theoretical limits of rapid sample transfer are close to being reached in these configurations, considering practical bounds on mechanical acceleration, and blotting or pressurization, respectively.^[63]
- c) **Triggered stimulation and cryo-arrest without observation:** Triggered cooling of the sample differs from the previous method, since the sample is not directly observed. By using a timed stimulus (e.g., optical, electric, or chemical signal), a dynamic process or function initiated by this signal can be narrowed down precisely. The key here is that simple trigger signals are more easily integrated directly into plunge freezing or HPF systems than full-featured light microscopic observation. First approaches started with electrical stimulation and sudden immersion in chemical fixative or cooling to observe synaptic vesicle exocytosis.^[64,65] More recently the method has evolved toward using optical or optogenetic signals, allowing to reach temporal resolution of up to ≈ 10 ms in high-pressure freezers,^[37,42,66,67] and up to 70 ms with plunge freezers.^[68] Drawbacks of the method are mainly two-fold: the necessity of the process to be triggered and the lack of prior observation. However, many biological processes, such as membrane trafficking in synapses can be specifically targeted and activated by optogenetics or electrical stimulation, making the method attractive for such applications. Devices that enable triggered

stimulation inside high-pressure freezers are now commercially available and have already led to many new discoveries mainly in the field of neuroscience.

- d) **Time-resolved chemical fixation:** Dynamic processes that cannot be triggered at a precise time can sometimes be slowed down or stopped in a well-defined state by chemical cross-linking. However, for imaging at the nanometer scale, fixation artefacts are a significant concern. Recent studies show that most fixatives such as formaldehyde create distinct displacement of proteins and lipids, including their loss from cells and that the full fixation process can take 4–60 min.^[69] Nevertheless, the possibility of following the process continuously with light microscopy can add substantial insight if the dynamics and size of the system are on the right scale. For example, Stepanek and Pignino employed this approach to great advantage to capture the direction of intraflagellar transport with total internal reflection fluorescence microscopy (TRIF) and to correlate this information with the ultrastructure using room temperature electron microscopy.^[6] These approaches show great potential to observe highly dynamic processes in the ≈ 500 ms range, where targeted stimulation of the process is not possible, but observation is required to functionally correlate EM images.

The idea of observing the sample cooling process itself with high temporal resolution would allow the finest temporal dynamics to be captured. With conventional methods for cryo-arresting samples, such as plunge-freezing, slam-freezing, or high-pressure freezing, the integration of a microscope and the observation of the process however become increasingly challenging. Therefore, different freezing approaches have been developed to allow for the integration of a light-microscope.

- e) **Cryofixation with observation by shifting the equilibrium temperature:** The approach consists of rapidly immersing the sample into or spraying it with a cryogenic fluid (e.g., liquid nitrogen) to effect rapid cooling from room temperature. The shift in thermal equilibrium is subsequently sustained by complete immersion in the cryogen. One advantage of using jet or spray freezing over plunging is that superior cooling rates are attainable due to the thinly squeezed thermal boundary layer.^[70] This is primarily a concern for biological samples. A second advantage of jet freezing is that it can work for larger, more complex sample carriers than bare TEM grids. For example, Huebinger et al. showed that a liquid nitrogen jet directed at a diamond heat sink can be used for cryo-arresting cells in an epifluorescence microscope.^[38] However, sample extraction to perform cryo-EM imaging has not yet been shown. The difficulty is symptomatic for a broader challenge in dynamic cryo-CLEM. Microscopic environments are needed that can 1) accommodate a close-to-native room-temperature model for the system of interest, 2) possess thermal time constants in the millisecond range, and 3) are electron transparent or can be made so using standard cryo-TEM and cryo-SEM preparation techniques.
- f) **Cryofixation with observation by collapse of a warm non-equilibrium state:** Another concept for observation of the cryofixation process itself is pre-cooling the setup to cryo-temperatures, while actively heating the sample to room tem-

perature. Then, with termination of the active heating, the thermal energy that is stored in the sample can be quickly depleted to a stable state, with millisecond duration of the transient and sub-millisecond time resolution for the time of cryo-arrest.^[39,71] As the cold state after cryo-fixation is the only stable equilibrium, the heater can, in principle, be turned on or off to produce warm-to-cold and cold-to-warm transitions with symmetric transients. However, active temperature regulation in the warm state is required. Sample extraction for cryo-EM has been achieved by FIB/SEM after lifting the sample off the inactive heater in a cryostat.

5. Outlook

There is a rapid growth in super resolution light microscopy and in electron microscopy techniques focusing on increased spatial resolutions. However, the dynamic nature of biological and other soft materials is pushing the limits of traditional sample preparation. We have investigated the current spatial and temporal limits of precision correlation between rapid perturbations and ultrastructural changes. In conclusion, the combined use of triggered and/or observed rapid cryofixation with electron microscopy fills a critical gap. While conventional in situ electron microscopy provides the most precise temporal and spatial correlation between structure and dynamics, additional methods are needed due to radiation sensitivity, lack of electron transparency, or insufficient vacuum compatibility of some systems. Prominent examples include biomaterials, battery materials, and organic nanoparticles, to name a few. For these applications, rapid fixation may sometimes offer an attractive compromise between dynamics and high-resolution structure. Among the possible fixation techniques, cryofixation is unique in that it works independent of the chemistry of the system under study. A limitation, however, is that only relatively thin samples can be preserved well.

Which applications may benefit from the advances in dynamic cryo-CLEM? First, many dynamic cellular processes at membranes, such as drug delivery, cell-to-cell-communication, or synaptic transmission involve ultrastructural dynamics on a millisecond timescale. Other aspects of rapid cellular dynamics on a sub-second timescale include intracellular transport processes, motility, and the rapid assembly of immunological synapses. Understanding the impressive interplay of molecular machines behind these complex processes is still an intensive matter of research. A second area is the growing field of biomaterials at the interface between synthetic, cell, and structural biology. For example, understanding controlled fission and fusion of membranes at a structural level will help to reconstitute similar functions in minimal artificial cells and organelles. This would be of great interest for applications in biotechnology and medical therapeutics. Methodological advances in sample preparation will allow such processes to be studied more precisely with adequate temporal sampling. In particular, this may help to better quantify their kinetics and to discover very short-lived intermediate states under native conditions.

In materials science, dynamics at the ultrastructural level is also of growing interest, for example for understanding the kinetics of dendrite formation in batteries, nanoparticle growth/dissolution, aggregation phenomena, drug release, and

the structural dynamics in soft materials such as gels. More than in biology, characterizing technical devices under operating conditions will require application-specific interfaces. While visual access is often needed, e.g. for microscopy, optical spectroscopy, or photocatalysis, the samples in materials science are not always transparent to visible light. At the same time, a variety of other physical interfaces, such as electrical connections, liquid or gas purging, and precision temperature control may need to be provided. A current frontier therefore is the development of application-specific multimodal testbeds for in situ EM and dynamic cryo-CLEM workflows.

When this is accomplished, a challenge affecting all applications is to expose locations of interest inside the frozen sample. The only exception are samples prepared by plunge freezing or jet freezing on TEM grids, which are already thin enough for cryo-TEM and cryo-STEM. Thicker samples require further preparation. Until the advent of cryo-focused ion beam milling (cryo-FIB), only ultramicrotomy and freeze fracture were available for exposing interior surfaces deep inside such bulky samples. However, cryo-FIB milling using conventional Gallium-ion beams is an option only if the region of interest is no more than a few micrometers from the surface. An exciting new development is therefore the emergence of a new generation of plasma-FIB (p-FIB) tools, which achieve drastically higher ablation rates than Gallium-ion FIB. Using p-FIB under cryogenic conditions opens a new perspective for analyzing specimens prepared by dynamic cryo-CLEM inside tens of micrometer thick microenvironments that are visually accessible and incorporate interfaces for complex interactive experiments.

With this in mind, we believe that a seamless integration of live imaging, sample manipulation, and rapid cryofixation into existing EM/TEM workflows will enable broader use and lead to new scientific discoveries in biology and materials science.

Supporting Information

Supporting Information is available from the Wiley Online Library or from the author.

Acknowledgements

This work is part of a project that received funding from the European Research Council (ERC) under the European Union's Horizon 2020 research and innovation programme (Grant agreement No. 772441).

Open access funding enabled and organized by Projekt DEAL.

Conflict of Interest

The authors declare no conflict of interest.

Keywords

CLEM, correlative microscopy, cryo-EM, vitrification

Received: November 3, 2023
Revised: March 17, 2024
Published online: April 16, 2024

- [1] F. M. Ross, *Science* **2015**, *350*, aaa9886.
- [2] H. Wu, H. Friedrich, J. P. Patterson, N. A. J. M. Sommerdijk, N. de Jonge, *Adv. Mater.* **2020**, *32*, 2001582.
- [3] H. Singh, K. A. Bishen, D. Garg, H. Sukhija, D. Sharma, U. Tomar, *Dent. J. Adv. Stud.* **2019**, *07*, 051.
- [4] I. Hurbain, M. Sachse, *Biol. Cell* **2011**, *103*, 405.
- [5] M. F. Hayles, D. A. M. de Winter, *J. Microsc.* **2021**, *281*, 138.
- [6] L. Stepanek, G. Pigino, *Methods in Cell Biol.* **2017**, *140*, 1.
- [7] M. Turk, W. Baumeister, *FEBS Lett.* **2020**, *594*, 3243.
- [8] R. K. Hylton, M. T. Swilius, *iScience* **2021**, *24*, 102959.
- [9] G. Zhao, J. Fu, *Biotechnol. Adv.* **2017**, *35*, 323.
- [10] Z. Han, A. E. Porter, *Front. Nanotechnol.* **2020**, *2*, 606253.
- [11] E. Brown, J. Mantell, D. Carter, G. Tilly, P. Verkade, *Semin. Cell Dev. Biol.* **2009**, *20*, 910.
- [12] A. J. Koster, J. Klumperman, *Nat. Rev. Mol. Cell Biol.* **2003**, *4*, SS6.
- [13] (Eds. P. Verkade, L. Collinson), in *Correlative Imaging: Focusing on the Future*, John Wiley & Sons Ltd., New York, USA **2020**.
- [14] Y. S. Bykov, M. Cortese, J. A. G. Briggs, R. Bartenschlager, *FEBS Lett.* **2016**, *590*, 1877.
- [15] Y. Li, W. Huang, Y. Li, W. Chiu, Y. Cui, *ACS Nano* **2020**, *14*, 9263.
- [16] E. Abbe, *Arch. für Mikroskopische Anat.* **1873**, *9*, 413.
- [17] Y. Eilers, H. Ta, K. C. Gwosch, F. Balzarotti, S. W. Hell, *Proc. Natl. Acad. Sci., USA* **2018**, *115*, 6117.
- [18] Y. Guo, D. Li, S. Zhang, Y. Yang, J.-J. Liu, X. Wang, C. Liu, D. E. Milkie, R. P. Moore, U. S. Tulu, D. P. Kiehart, J. Hu, J. Lippincott-Schwartz, E. Betzig, D. Li, *Cell* **2018**, *175*, 1430.
- [19] W. Zhao, S. Zhao, L. Li, X. Huang, S. Xing, Y. Zhang, G. Qiu, Z. Han, Y. Shang, D.-E. Sun, C. Shan, R. Wu, L. Gu, S. Zhang, R. Chen, J. Xiao, Y. Mo, J. Wang, W. Ji, X. Chen, B. Ding, Y. Liu, H. Mao, B.-L. Song, J. Tan, J. Liu, H. Li, L. Chen, *Nat. Biotechnol.* **2022**, *40*, 606.
- [20] A. Chmyrov, J. Keller, T. Grotjohann, M. Ratz, E. d'Este, S. Jakobs, C. Eggeling, S. W. Hell, *Nat. Methods* **2013**, *10*, 737.
- [21] V. Westphal, S. O. Rizzoli, M. A. Lauterbach, D. Kamin, R. Jahn, S. W. Hell, *Science* **2008**, *320*, 246.
- [22] H. Deschout, T. Lukes, A. Sharipov, D. Szlag, L. Feletti, W. Vandenberg, P. Dedecker, J. Hofkens, M. Leutenegger, T. Lasser, A. Radenovic, *Nat. Commun.* **2016**, *7*, 13693.
- [23] L. Zhu, W. Zhang, D. Elnatan, B. Huang, *Nat. Methods* **2012**, *9*, 721.
- [24] C. A. Larabell, K. A. Nugent, *Curr. Opin. Struct. Biol.* **2010**, *20*, 623.
- [25] D. R. Spitz, E. I. Azzam, J. J. Li, D. Gius, *Cancer Metastasis Rev.* **2004**, *23*, 311.
- [26] N. De Jonge, D. B. Peckys, *ACS Nano* **2016**, *10*, 9061.
- [27] S. Waldchen, J. Lehmann, T. Klein, S. Van De Linde, M. Sauer, *Sci. Rep.* **2015**, *5*, 15348.
- [28] T. R. Shaikh, A. S. Yassin, Z. Lu, D. Barnard, X. Meng, T.-M. Lu, T. Wagenknecht, R. K. Agrawal, *Proc. Natl. Acad. Sci., USA* **2014**, *111*, 9822.
- [29] P. G. Debenedetti, *J. Phys. Condens. Matter* **2003**, *15*, R1669.
- [30] H. Mikami, J. Harmon, H. Kobayashi, S. Hamad, Y. Wang, O. Iwata, K. Suzuki, T. Ito, Y. Aisaka, N. Kutsuna, K. Nagasawa, H. Watarai, Y. Ozeki, K. Goda, *Optica* **2018**, *5*, 117.
- [31] F. Huang, T. M. P. Hartwich, F. E. Rivera-Molina, Y. Lin, W. C. Duim, J. J. Long, P. D. Uchil, J. R. Myers, M. A. Baird, W. Mothes, M. W. Davidson, D. Toomre, J. Bewersdorf, *Nat. Methods* **2013**, *10*, 653.
- [32] N. Strelnikova, N. Sauter, M. Guizar-Sicairos, M. Göllner, A. Diaz, P. Delivani, M. Chacón, I. M. Tolic, V. Zaburdaev, T. Pfohl, *Sci. Rep.* **2017**, *7*, 13775.
- [33] T. Ando, N. Kodera, E. Takai, D. Maruyama, K. Saito, A. Toda, *Proc. Natl. Acad. Sci., USA* **2001**, *98*, 12468.
- [34] R. Schmidt, T. Weihs, C. A. Wurm, I. Jansen, J. Rehman, S. J. Sahl, S. W. Hell, *Nat. Commun.* **2021**, *12*, 1478.
- [35] A. Sartori-Rupp, D. Cordero Cervantes, A. Pepe, K. Gousset, E. Delage, S. Corroyer-Dulmont, C. Schmitt, J. Krijnse-Locker, C. Zurzolo, *Nat. Commun.* **2019**, *10*, 342.
- [36] P. Verkade, *J. Microscopy* **2007**, *230*, 317.
- [37] S. Watanabe, *Front. Synaptic Neurosci.* **2016**, *8*, 4024.
- [38] J. Huebinger, H. Grecco, M. E. Masip, J. Christmann, G. R. Fuhr, P. I. H. Bastiaens, *Sci. Adv.* **2021**, *7*, 882.
- [39] M. Fuest, G. M. Nocera, M. M. Modena, D. Riedel, Y. X. Mejia, T. P. Burg, *J. Microsc.* **2018**, *272*, 87.
- [40] Digital Science, "Dimensions[Software]" <https://app.dimensions.ai> (accessed: October 2023).
- [41] J. M. Plitzko, A. Rigort, A. Leis, *Curr. Opin. Biotechnol.* **2009**, *20*, 83.
- [42] S. Watanabe, M. Davis, E. Jorgensen, *Nanoscale Imaging of Synapses*, Part of the Neuromethods Book Series, Humana Press, New York, NY **2014**, 84.
- [43] W. B. Bald, *J. Microsc.* **1986**, *143*, 89.
- [44] N. H. Fletcher, *Reports Prog. Phys.* **1971**, *34*, 913.
- [45] J. Huebinger, H. M. Han, O. Hofnagel, I. R. Vetter, P. I. H. Bastiaens, M. Grabenbauer, *Biophys. J.* **2016**, *110*, 840.
- [46] A. Leforestier, K. Richter, F. Livolant, J. Dubochet, *J. Microsc.* **1996**, *184*, 4.
- [47] K. Semmler, J. Wunderlich, W. Richter, H. W. Meyer, *J. Microscopy* **1998**, *190*, 317.
- [48] C. Blancard, B. Salin, *J. Vis. Exp.* **2017**, *1*, <https://doi.org/10.3791/54874>.
- [49] J. Dubochet, A. W. McDowell, *J. Microsc.* **1981**, *124*, 3.
- [50] L. V. Bock, H. Grubmüller, *Nat. Commun.* **2022**, *13*, 1709.
- [51] J. Escaig, *J. Microsc.* **1982**, *126*, 221.
- [52] Y. Akiyama, M. Shinose, H. Watanabe, S. Yamada, Y. Kanda, *Proc. Natl. Acad. Sci., USA* **2019**, *116*, 7738.
- [53] M. Fuest, M. Schaffer, G. M. Nocera, R. I. Galilea-Kleinsteuber, J.-E. Messling, M. Heymann, J. M. Plitzko, T. P. Burg, *Sci. Rep.* **2019**, *9*, 1.
- [54] Y. X. Mejia, H. Feindt, D. Zhang, S. Steltenkamp, T. P. Burg, *Lab Chip* **2014**, *14*, 3281.
- [55] R. Dahl, L. A. Staehelin, *J. Electron Microsc. Tech.* **1989**, *13*, 165.
- [56] D. Studer, B. M. Humbel, M. Chiquet, *Histochem. Cell Biol.* **2008**, *130*, 877.
- [57] E. M. Mandelkow, E. Mandelkow, R. A. Milligan, *J. Cell Biol.* **1991**, *114*, 977.
- [58] W. Li, J. Lu, K. Xiao, M. Zhou, Y. Li, X. Zhang, Z. Li, L. Gu, X. Xu, Q. Guo, T. Xu, W. Ji, *Nat. Methods* **2023**, *20*, 268.
- [59] S. Li, X. Jia, T. Niu, X. Zhang, C. Qi, W. Xu, H. Deng, F. Sun, G. Ji, *Commun. Biol.* **2023**, *6*, 474.
- [60] S. Li, Z. Wang, X. Jia, T. Niu, J. Zhang, G. Yin, X. Zhang, Y. Zhu, G. Ji, F. Sun, *Nat. Methods* **2023**, *20*, 276.
- [61] R. I. Koning, F. G. Faas, M. Boonekamp, B. de Visser, J. Janse, J. C. Wiegant, A. de Breij, J. Willemsse, P. H. Nibbering, H. J. Tanke, A. J. Koster, *Ultramicroscopy* **2014**, *143*, 67.
- [62] X. Heiligenstein, M. de Beer, J. Heiligenstein, F. Eyraud, L. Manet, F. Schmitt, E. Lamers, J. Lindenau, M. Kea-te Lindert, J. Salamero, G. Raposo, N. Sommerdijk, M. Belle, A. Akiva, in *Correlative Light and Electron Microscopy IV*, (Eds. T. Müller-Reichert, P. Verkade), Academic Press, Cambridge, Massachusetts **2021**, 162, 115.
- [63] D. Cheng, M. D. R. Graham, S. Dar-Bieh, B. Filip, *Formatex Book Series 5*, Chapter: Current Microscopy Contributions to Advan, Formatex, Badajoz, Spain **2012**.
- [64] J. E. Heuser, T. S. Reese, *J. Cell Biol.* **1973**, *57*, 315.
- [65] C. L. Schwartz, V. I. Sarbash, F. I. Ataullakhanov, J. R. McIntosh, D. Nicastro, *J. Microsc.* **2007**, *227*, 98.
- [66] C. Borges-Merjane, O. Kim, P. Jonas, *Neuron* **2020**, *105*, 992.
- [67] C. Imig, F. J. López-Murcia, L. Maus, I. H. García-Plaza, L. S. Mortensen, M. Schwark, V. Schwarze, J. Angibaud, U. V. Nägerl, H. Taschenberger, N. Brose, B. H. Cooper, *Neuron* **2020**, *108*, 843.
- [68] N. Yoder, F. Jalali-Yazdi, S. Noreng, A. Houser, I. Bacongus, E. Gouaux, *J. Struct. Biol.* **2020**, *212*, 107624.
- [69] J. Huebinger, J. Spindler, K. J. Holl, B. Koos, *Sci. Rep.* **2018**, *8*, 17756.

- [70] R. B. G. Ravelli, F. J. T. Nijpels, R. J. M. Henderikx, G. Weissenberger, S. Thewessem, A. Gijsbers, B. W. A. M. M. Beulen, C. López-Iglesias, P. J. Peters, *Nat. Commun.* **2020**, *11*, 2563.
- [71] T. P. Burg, Max Planck Gesellschaft zur Foerderung der Wissenschaften eV, US8256232B2 **2012**.
- [72] S. W. Hell, J. Wichmann, *Opt. Lett.* **1994**, *19*, 780.
- [73] E. Betzig, G. H. Patterson, R. Sougrat, O. W. Lindwasser, S. Olenych, J. S. Bonifacino, M. W. Davidson, J. Lippincott-Schwartz, H. F. Hess, *Science* **2006**, *313*, 1642.
- [74] T. Sulchek, R. Hsieh, J. D. Adams, S. C. Minne, C. F. Quate, D. M. Adderton, *Rev. Sci. Instrum.* **2000**, *71*, 2097.
- [75] W. Chao, B. D. Harteneck, J. A. Liddle, E. H. Anderson, D. T. Attwood, *Nature* **2005**, *435*, 1210.
- [76] J. Park, H. Park, P. Ercius, A. F. Pegoraro, C. Xu, J. W. Kim, S. H. Han, D. A. Weitz, *Nano Lett.* **2015**, *15*, 4737.
- [77] M.-E. Mäeots, B. Lee, A. Nans, S.-G. Jeong, M. M. N. Esfahani, S. Ding, D. J. Smith, C.-S. Lee, S. S. Lee, M. Peter, R. I. Enchev, *Nat. Commun.* **2020**, *11*, 3465.